THE ASTRONOMICAL JOURNAL VOLUME 103, NUMBER 6 JUNE 1992

BAR STAR CLUSTERS IN THE LMC: FORMATION HISTORY FROM *UBV* INTEGRATED PHOTOMETRY

E. BICA[1,2]

Instituto de Física, Universidade Federal do Rio Grande do Sul, Av. Bento Gonçalves 9500, 91500, Porto Alegre, RS, Brazil

J. J. CLARIÁ[2]

Observatorio Astronómico, Universidad Nacional de Córdoba, Laprida 854, 5000 Córdoba, Argentina

H. DOTTORI[2]

Instituto de Física, Universidade Federal do Rio Grande do Sul, Av. Bento Gonçalves 9500, 91500, Porto Alegre, RS, Brazil

Received 1 May 1991; revised 11 February 1992

ABSTRACT

The sample of star clusters in the LMC Bar region with integrated *UBV* photometry was enlarged by approximately a factor 4, totalling 129 objects. The $(B-V)$ histogram gap between blue and red clusters disappears with this deeper sample. Age groups in terms of equivalent SWB types were derived and their spatial distribution studied. Clusters younger than $t\approx 200$ Myr are not homogeneously distributed through the bar. In particular a strong star forming event at $t\approx 100$ Myr was detected in the eastern part of the Bar, consisting of a compact grouping of seven coeval clusters around NGC 2058 and NGC 2065. We also analyze 11 close pairs and two trios, and the colors indicate that only four pairs are clearly not coeval.

1. INTRODUCTION

It is known since quite long that the Magellanic Clouds contain rich star clusters of all ages (Hodge 1960, 1961). Many studies of HR diagrams and integrated photometry were made in subsequent years. The integrated *UBV* photometry of 61 SMC clusters and 147 LMC star clusters was compiled by Van den Bergh (1981, hereafter referred to as VDB81). He analyzed the overall spatial distribution in terms of four age groups and concluded, for the LMC, that very young clusters are concentrated in Shapley's constellations and the centroid of old clusters is displaced from the Bar. The sample, which consists mostly of bright objects, presents a rather clear-cut gap in the $(B-V)$ histogram between blue and red clusters, for both clouds. The gap has been interpreted as a consequence of disruption of less massive clusters as they approach intermediate ages and/or fading of clusters below the survey limit owing to stellar evolution effects.

Ever since, some new observations have been published: Gordon & Kron (1983) have made multiaperture photometry but no new entries were added to VDB81's list; Bica *et al.* (1986, hereafter referred to as BDP86) have observed in *BV* some of VDB81 clusters and 27 previously unstudied ones fainter than $V\approx 13.0$ in the SMC. They found that many of them tend to fulfill the gap in the SMC $(B-V)$ histogram. Mateo (1987) observed in *UBV* a deep sample of 29 clusters in a remote northern region of the LMC. His sample resulted predominantly red, whereas that of VDB81 is dominated by blue clusters. Consequently spatial variations in cluster ages appear to occur in the LMC.

Other studies have reanalyzed the existing samples providing age calibrations and discussing whether the $(B-V)$ gap can be explained or not by enhanced epochs of star formation (e.g., Chiosi *et al.* 1988, hereafter referred to as CBB88). Care must be taken in drawing conclusions about age distributions directly from $(B-V)$ histograms. Because of the way the clusters lie in the $(U-B)-(B-V)$ plane, even a sample distributed uniformly along an age sequence would, when projected onto the $B-V$ axis, produce a histogram with a gap.

The need of new observations in order to clarify the nature of the color histogram and its relationship to the spatial distribution is evident. With this in mind, we have started a deep *UBV* survey of cloud clusters, presenting in this paper the results for a new sample of 95 clusters in the Bar region of the LMC. This sample seems to be mostly physically connected to the Bar (Sec. 2) and, consequently, we are probing the history of star formation of the Bar itself. Also, it should be possible to get some clues on the dynamical origin of the Bar.

A deep *UBV* survey is important as a solid database for object selection in more detailed future studies with techniques which require longer exposures, such as (i) CCD photometry for HR diagrams (e.g., Mateo *et al.* 1986; Mould *et al.* 1986); (ii) narrowband integrated photometry like the *G* band and Hβ one for red clusters (BDP86), which is very sensitive to metallicity and age; (iii) CCD photometry for metallicity determinations of individual stars in clusters, e.g., the Washington photometry system (Geisler 1987); and (iv) identification of old clusters which are candidates for RR Lyrae surveys (Graham & Nemec 1984).

[1]Visiting Astronomer, Cerro Tololo Inter-American Observatory supported by the National Science Foundation under Contract No. AST-74-041-128.

[2]Visiting Astronomer, Complejo Astronómico El Leoncito operated under agreement between the Consejo Nacional de Investigaciones Científicas y Técnicas de la República Argentina and the National Universities of La Plata, Córdoba and San Juan, Argentina.

 0004-6256/92/061859-13$00.90

In Sec. 2 we present the observations and analyze the error sources. In Sec. 3 we discuss the results, particularly the $(B-V)$ histogram and the spatial distribution of different age groups. We compare the colors in pairs, trios, and a compact grouping of eight clusters in Sec. 4. Finally, the main conclusions are summarized in Sec. 5.

2. THE OBSERVATIONS

2.1 The Sample and its Relation to the Bar

The sample was selected on B, J, R, and I Sky Survey Schmidt plates, guided by identifications in Hodge & Wright's (1967) atlas, as well as by coordinates, descriptions and plate identifications in catalogs of star clusters, stellar associations, and emission nebulae. The objective was to establish a considerably deeper sample as compared to that of VDB81. The acronyms for catalogs and their references are indicated in Tables 1–3, for the final ensemble of bar objects. During this search we cross checked catalogs and the atlas, and a possible misidentification was clarified (see note c in Table 1).

We found a cluster which appears to have been overlooked in past searches. It is labelled in Table 1 according to its approximate 1950 coordinates: ANON $5^h21.7^m$-69°27′. This cluster should not be confused with the nearby ones HS243 and HS245. The *UBV* results (Sec. 3) suggest that it belongs to the stellar association LH46.

The objects observed for the first time in *UBV* photometry total 95 and are listed in Table 1. Table 3 contains the clusters in VDB81's compilation which appear to have well-established magnitude and colors according to his analysis of consistency between results in different sources: such clusters (23) *were not* reobserved and we use in the subsequent analysis the values from VDB81. Table 2 lists the objects which had uncertain or incomplete photometry according to VDB81, and/or those which had been observed with inadequate diaphragms with respect to object size. Such clusters (11) were reobserved, and the values given in Table 2 are the *new* ones. We thus emphasize that Table 2 should not be used as test of agreement with previous photometries. A detailed discussion of the revised values is provided in Sec. 2.3.

We show in Fig. 1 the positions of all clusters in the SL (Shapley & Lindsay 1963) and HS (Hodge & Sexton 1966) catalogs in a region 3°×5° containing the Bar. Although there exist deeper catalogs in particular regions (e.g., Hodge 1988), the merge of the SL and HS catalogs is the most homogeneous list available for the Bar region and surroundings at the present time. The cluster density is a factor $\approx$2.5 larger in the Bar region with respect to the surroundings, which suggests that $\approx$3/5 of them are physically connected to the Bar, rather than simply projected on it. Missing clusters are expected in the Bar because the background is brighter, but outside the Bar some large H II region complexes contribute to a lower detection rate too. Deep searches over the whole region and quantitative analyses are necessary to check these points further.

The rectangle in Fig. 1 encompasses the LMC Bar as seen on photographic plates. The 129 star clusters that we analyse (Tables 1–3) are the brightest objects in that zone. The cluster brightness in the Sky Survey Plates provided a means to select the clusters observable in the available telescopes. The study of clusters in the Bar region might give information on the history of the Bar itself.

2.2 Photometric Data and Error Analysis

Most of the photoeletric observations here reported were carried out with standard *UBV* filters and the 61 cm Lowell telecope at the Cerro Tololo Inter-American Observatory (CTIO) during eight nights in December 1989, complemented with additional observations in November 1990 and January 1991. A dry-ice cold box with a phototube EMI 9781 A was employed. The *U* filter was blocked with a 2 mm solid crystal of $CuSO_4$ in order to suppress the red leak.

We describe in detail December 1989's run, during which most of the present observations were collected. The standard stars observed were C, F, N, P, Q, and S from the E2 region and HD 49798 from E3 (Graham 1982), spanning the range $-0.29 < (B-V) < 1.61$. HD 49798 is extremely important to derive reliable colors for very young clusters embedded in H II regions. In addition, we have observed a blue and a red star in the LMC at different airmasses for a nightly determination of the extinction coefficients. Typical values obtained were $K_V = 0.23$, $K_{BV} = 0.13$, and $K_{UB} = 0.31$, i.e., somewhat above the average values for CTIO. These stars are numbers 1 and 2 in the Bok and Tifft sequence, as revised by Alcaino & Liller (1982), and were also used as a check for the transformations to the standard system. The slopes of the linear relations in the color transformations were found to be within 7% of unity, while the color term for the *V* magnitude transformation turned out to be about 0.014 $(B-V)$. The typical nightly rms of differences between standard and transformed values were $\sigma_V = 0.008$, $\sigma_{B-V} = 0.004$, and $\sigma_{U-B}=0.022$.

Applying the standard system transformation to the blue and red LMC stars discussed above, we obtain systematic differences which are smaller than 0.007 in all indices, between us and Alcaino & Liller (1982). The results for these stars, which were observed several times each night at airmasses comparable to those of the star clusters, allow us to conclude that the standard *UBV* system has been well reproduced during the observing run.

The observations of the star clusters consisted of 30 s integrations for cluster and sky regions until 1% precision was attained. In general this was achieved with two integrations owing to the photometric quality of the nights. The adoption of this procedure yielded internal errors which are shown in Fig. 2. We conclude that observations of extended objects with this telescope, auxiliary equipment, and integration time, are appropriate for $V < 13.2$ and that this limit is established by the errors in the $(U-B)$ color.

The sky region for each cluster was chosen on plates, and checked again at the telescope, in order to avoid contamination of atypically bright field stars. In addition, for

TABLE 1. New sample of star clusters.[a]

Name	D(")	V	B-V	U-B	SWB	Remarks
SL180	38C	13.49	0.66	0.18	V	
SL181	38C	13.21	0.45	0.03	IVA	
SL191	40	12.16	0.35	-0.24	I	in LH16
NGC1825,SL202	34	12.04	0.41	-0.26	I	
SL212	100	12.20	0.18	-0.24	II	
SL218	100	12.24	0.13	-0.34	I	
NGC1836,SL223	50	12.22	0.28	0.02	III	
NGC1838,SL225	50	12.93	0.27	-0.23	II	
NGC1839,SL226	50	11.80	0.10	-0.18	II	
HS109	50	12.52	0.11	-0.26	II	
HS117	50	13.00	0.67	0.34	V	
SL229	50	13.28	0.33	0.24	IVA	pair with SL230
SL230	50	11.34	0.29	-0.35	I	pair with SL229
SL234	40	12.44	-0.03	-0.36	II	
SL237	50	11.27	0.42	-0.16	II	in LH27
SL244	40	13.04	0.77	0.13	VII	
SL250	34	13.15	0.59	0.21	IVB	
NGC1850A	25	11.23	-0.14	-0.89	0	(b)
H88-159	40	11.84	0.14	-0.41	I	(b)
SL260	38C	13.15	0.34	-0.06	III	
SL268	50	12.16	0.66	0.33	V	
SL276	40	12.95	0.45	0.19	IVB	pair with SL280
SL278	38C	13.63	0.50	-0.02	IVA	
SL280	150	11.92	0.27	-0.61	I	pair with SL276
SL288	34	12.06	-0.03	-0.40	I	
SL296	34	13.10	0.42	0.12	IVA	
SL304	40	12.99	0.33	-0.05	III	
NGC1865,SL307	40	12.91	0.69	0.08	VII	
NGC1874,HEN113D	50	12.81	-0.34	-1.03	0	in SL320,in LH35,pair/76
NGC1876,HEN113C	50	11.71	-0.17	-1.00	0	in SL320,in LH35,pair/74
SL320,NGC1874-6-7	150	10.34	-0.20	-1.02	0	HEN113A-B-C-D-E,in LH35
SL328,LH39	100	10.86	0.03	-0.74	I	
NGC1894,SL344	34	12.16	0.24	-0.21	II	
SL349	50	13.27	0.62	0.34	V	pair with H1
H1,SL353	50	12.40	0.66	0.27	V	pair with SL349
SL357	38C	13.30	0.64	0.29	V	pair with NGC1903
SL358	40	13.10	0.40	0.09	IVA	
H88-266,in LH41	100	10.98	-0.06	-0.86	0	in HEN119,pair w H88-267
H88-267,in LH41	100	9.09	0.11	-0.69	I	in HEN119,incl S Dor
SL368	50	13.03	0.52	0.22	IVB	

TABLE 1. (continued)

Name	D(")	V	B-V	U-B	SWB	Remarks
NGC1921W,HEN121	34	13.21	0.02	-0.81	0	pair with NGC1921E
NGC1921E,SL381	34	12.95	0.19	-0.21	II	pair with NGC1921W
SL385	40	12.78	0.37	0.07	IVA	pair with SL387
SL387	40	13.07	0.44	0.08	IVA	pair with SL385
SL390	100	12.53	0.52	-0.03	IVA	
	34	13.46	0.50	-0.10		
NGC1922,SL391	34	11.51	0.13	-0.41	I	
SL397	34	12.22	0.12	-0.37	I	
NGC1926,SL403	40	11.79	0.26	-0.09	III	(c)
NGC1928,SL405,HS243	34	12.47	0.71	0.07	VII	(c)
ANON 5h21.7m-69°27'	40	13.49	-0.22	-0.94	0	in LH46,not HS245/HS243
SL412	40	13.17	0.30	-0.09	III	
NGC1938,SL413	34	12.91	0.49	0.08	IVA	pair with NGC1939
	38C	13.09	0.45	0.01		
NGC1939,SL414	34	11.83	0.69	0.10	VII	pair with NGC1938
	38C	11.78	0.70	0.08		
SL418	40	12.82	0.19	-0.06	III	
SL419	40	12.70	0.23	0.00	III	
HS248,HEN127A	50	12.70	-0.25	-1.04	0	
SL423	40	12.69	0.13	-0.24	II	
NGC1950,SL450	40	13.17	0.54	0.22	IVB	
SL453	40	12.27	0.30	-0.05	III	
NGC1958,SL462	34	12.99	0.54	0.03	IVA	
NGC1959,SL466	34	12.17	0.38	-0.03	IVA	
SL468	40	12.42	0.15	-0.13	III	
HS298	25	12.59	0.47	-0.53	I	
SL475,LH57,HEN143	100	11.52	-0.20	-0.93	0	
NGC1969,SL479	40	12.46	0.20	-0.15	III	triple with NGC1971/2
NGC1971,SL481	34	11.90	0.11	-0.26	II	triple with NGC1969/72
NGC1972,SL480	34	12.62	0.33	-0.20	II	triple with NGC1969/71
SL508	40	11.92	0.21	-0.25	II	
SL528	40	13.32	0.52	0.29	IVB	
SL535	40	13.20	0.04	-0.31	II	
SL542	40	12.59	0.43	-0.02	IVA	
SL558	40	13.12	0.18	0.04	III	
SL574	40	12.81	0.23	-0.14	III	pair with NGC2028
NGC2028,SL575	40	12.88	0.28	0.04	III	pair with SL574
NGC2033,in SL589	40	11.63	-0.10	-0.91	O	in LH81,in HEN154
NGC2036,SL587	40	12.77	0.19	-0.10	III	
NGC2037	150	10.31	-0.10	-0.83	0	in LH81,in HEN154
NGC2038,SL590	40	11.92	0.18	-0.21	II	
SL591	40	12.88	0.30	-0.10	III	
NGC2046,SL597	40	12.64	0.31	-0.07	III	
SL598	40	13.46	0.61	0.18	IVB	

TABLE 1. (continued)

Name	D(")	V	B-V	U-B	SWB	Remarks
SL599	40	13.17	0.04	-0.25	II	
NGC2047,SL600	40	13.15	0.23	-0.24	II	
LH87S	150	10.48	0.07	-0.79	0	in HEN154
NGC2048,LH87N,HEN154A	50	12.17	-0.12	-0.99	0	
NGC2057,SL616	40	12.17	0.22	-0.13	III	
NGC2059,SL613	40	12.85	0.31	-0.09	III	pair with NGC2058
NGC2066,SL627	40	13.10	0.35	-0.08	III	
NGC2072,SL630	40	13.21	0.52	0.04	IVA	
NGC2075,SL631,HEN213	100	11.47	0.01	-0.77	0	
SL636	40	13.54	0.31	0.11	IVA	
NGC2079,HEN159A	50	11.81	-0.12	-0.59	0	in SL644, in LH105
SL654	40	12.85	0.23	-0.13	III	
SL676	100	13.03	0.67	0.38	V	
	40	13.16	0.57	0.42		
SL740	40	13.54	0.54	0.24	IVB	

Notes to Table 1

[a] By columns: (1) star cluster designations: SL (Shapley and Lindsay, 1963), H (Hodge, 1960), HS (Hodge and Sexton, 1966), H88 (Hodge, 1988), related emission nebulae HEN (Henize, 1956) and associations LH (Lucke and Hodge, 1970); (2) diaphragm diameter in arc seconds, attached C are observations from CASLEO; (3), (4) and (5) magnitudes and colors V, (B-V) and (U-B) respectively; (6) equivalent SWB classification (Searle, Wilkinson and Bagnuolo (1980); (7) Note indications and remarks.

[b] NGC 1850, NGC 1850A and H88-159 are three components of a multiple cluster. NGC 1850A is the companion of NGC 1850 discussed in Bhatia and MacGillivray (1987). The colours of NGC1850A indicate that it is responsible for the ionization of the emission nebula surrounding the system. We have reobserved NGC 1850 with a 50" diaphragm (Table 2), whereas the observation quoted in VDB81 with 88" includes NGC 1850A and part of H88-159.

[c] There is confusion in the literature concerning the identification of NGC1926 and NGC1928. The original NGC and SL descriptions and positions are compatible with the following interpretation which we have adopted: in the Hodge and Wright Atlas (1967) and in Hodge (1988) NGC1926 is labelled as NGC1928, NGC1928 as HS243 and the object indicated in the atlas as NGC1926 is a star. The UBV observation of NGC1928 shown in VDB81 certainly refers to NGC1926.

the clusters H2=SL363, SL418, NGC 1926, and NGC 1928, which are located in the most crowded zones of the LMC Bar, we have observed two or three selected regions around each cluster, in order to estimate magnitude and color errors introduced by background variations in such particularly difficult zones. The average values of these errors in the object minus sky results are $\Delta_V = 0.036$, $\Delta_{B-V} = 0.017$, and $\Delta_{U-B} = 0.030$, which are suitable for our purposes. Although the Bar stars produce a bright background, it is locally quite homogeneous. Indeed atypically bright stars in background fields are more frequent in Shapley's Constellations than in the Bar.

Observations were repeated for 17 star clusters in two different nights throughout the observing run, and the agreement is better than 0.04 in all indices.

The CTIO observations were supplemented with *UBV* measurements of eight Bar clusters performed with the Boller and Chivens 2.14 m telescope at the Complejo Astronómico El Leoncito (CASLEO) in San Juan (Argentina) in February 1990, during a run of 6 nights dedicated to clusters in the external regions of the LMC. This telescope was equipped with the Vatican Observatory Polarimeter, VATPOL (Magalhães *et al.* 1984), used as a photoelectric photometer. Essentially the same procedure as that in CTIO was employed. A detailed analysis of the CASLEO observations will be presented elsewhere.

The results for the integrated magnitudes and colors obtained at CTIO and CASLEO, together with the diaphragm diameter through which each cluster was measured, are given in Tables 1 and 2. The observations from

TABLE 2. Revised values for 11 objects in VDB81.[a]

Name	D(")	V	B-V	U-B	SWB	Remarks
NGC1850,SL261	50	9.57	0.15	-0.27	II	
NGC1858,SL274,HEN105A	150	9.88	-0.12	-0.90	0	LH31
NGC1898,SL350	40	11.86	0.76	0.08	VII	
SL360	100	9.54	-0.15	-0.91	0	in LH41, in HEN119
SL362	50	11.48	0.11	-0.75	I	
H2,SL363	40	12.32	0.57	0.25	V	
NGC1910,SL371	150	9.65	-0.15	-0.88	0	in LH41, in HEN119
NGC1917,SL379	50	12.33	0.57	0.20	IVB	
NGC1918,LH42,HEN120	150	9.78	0.03	-0.93	0	
SL393	38C	12.61	0.41	-0.43	I	with RSG
	25C	13.43	-0.02	-0.60		without RSG
NGC2056,SL611	150	11.77	0.03	-0.12	III	

Note to Table 2
[a]column descriptions as in Table 1.

CASLEO are denoted by the letter C in the diaphragm column.

2.3 Discussion of Clusters with Revised Photometry

A comparison of the revised values in Table 2 with those in VDB81 deserves the following remarks: (a) We observed NGC 1850 with a smaller diaphragm to avoid contamination from the compact bluer companion NGC 1850 A. As expected, the revised colors for NGC 1850 are slightly redder, and the V magnitude is fainter. (b) NGC 1858, NGC 1910, and NGC 1918 are large complexes of H II region and OB association. Our diaphragms are larger than those in VDB81 because we intended to have global magnitude and colors for gas and stars. SL360 is a blue cluster attached to the NGC 1910 complex; SL362 is as well very blue. Our colors result $\approx$0.15 mag bluer on average for these objects relative to those listed in VDB81. This might arise from the relative spatial distribution of gas and stars in the complexes, or from the distribution of bright blue and red supergiants in clusters around 10 Myr old. However, the observation of a hot standard star is crucial in order to avoid calibration extrapolations for such extremely blue colors. We are confident in our results by the use of HD 49798. (c) Magnitude and colors of SL393 are dependent on the inclusion or not of a red supergiant at the cluster edge (Sec. 3). (d) NGC 1898 and H2=SL363 are in regions of strong background. VDB81 pointed out that the $(U-B)$ color for NGC 1898 might have been background affected. Our new value is 0.11 redder in $(U-B)$, placing the cluster in agreement with other type VII ones in the color–color diagram. Our colors for SL 363 result compatible with those in VDB81, within error bars and we also provide its magnitude which was lacking in VDB81. (e) NGC 2056 was reobserved because the diaphragm in VDB81 (25") was excessively small for the cluster size. The new value results 0.57 mag brighter in V, as expected, but the colors are considerably bluer. We have observed the cluster in two different nights with similar results. A color gradient produced by concentration of some bright red stars near the cluster center might explain the difference. (f) The value $V=10.25$ in VDB81's Table III for NGC 1917 suggests a misidentication in one of the compilation sources, and in addition the $(U-B)$ color was indicated as uncertain in that paper. Our revised values imply an equivalent SWB type IVB (Sec. 3), in agreement with that derived from the intermediate band photometry of BDP86. Moreover, the revised magnitude $V=12.33$ is expected from the cluster appearance on Sky Survey Plates, whereas the previous value was too bright.

3. ANALYSIS OF THE *UBV* RESULTS

3.1 Magnitude and Color Statistics and the Age Groups

The number of star clusters in different V magnitude intervals is shown in Fig. 3. We distinguish the old sample (Tables 2 and 3) from the new one. The new sample populates mostly the region $12.0 < V < 13.4$. The diagram behavior suggests that the sample is basically complete up to $V \simeq 13.2$, because the number of clusters falls off dramatically for fainter magnitudes. From our inspections of the Sky Survey plates and the catalogs (Sec. 2.1), no significant number of clusters brighter than $V \approx 13.0$ could have been missed; the only new cluster detected (Table 1) is fainter than this limit and the remaining ones in catalogs are apparently too faint on the plates.

Homogeneous estimates of cluster diameter available in the SL catalog, when compared to the diaphragm diameters in Tables 1 and 2, provide a mean ratio of 1.2, which ensures that we have measured essentially all the cluster light.

The Bar $(B-V)$ color histogram provided in Fig. 4(a), shows that when fainter clusters are included, as we did, the gap between blue and red clusters (VDB81, CBB88) in

TABLE 3. Equivalent SWB types derived from VDB81's *UBV* data.[a]

Name	SWB
NGC1804,SL172	II
NGC1828,SL203	III
NGC1830,SL207	IVA
NGC1834	I
NGC1835,SL215	VII
NGC1847,SL240	I
NGC1854,SL265	II
NGC1856,SL271	IVA
NGC1860,SL284	I
NGC1863,SL299	I
NGC1870,SL317	II
NGC1872,SL318	IVA
NGC1885,SL340	III
NGC1903,SL356[b]	II
NGC1913,SL373	II
NGC1916,SL361	VII
NGC1943,SL430	II
NGC1986,SL489	II
NGC2005,SL518	VII
NGC2019,SL554	VII
NGC2058,SL614[c]	III
NGC2065,SL626	III
NGC2107,SL629	IVA

Notes to Table 3

[a]By columns:
(1) Star cluster designation;
(2) equivalent SWB type
[b]pair with SL357
[c]pair with NGC2059

the region $0.4 < (B-V) < 0.6$, disappears. For comparison purposes we recall in Fig. 4(b) the histogram for the total LMC sample from VDB81. The numerous clusters which fulfill the gap in Fig. 4(a) have $(B-V)$ colors which agree with the typical color of the Bar stellar population $(B-V) \simeq 0.49$ (de Vaucouleurs & de Vaucouleurs 1959, and references therein). The color range $0.4 \leqslant (B-V) \leqslant 0.6$ corresponds basically to intermediate age clusters and the conclusion that they are common as one probes fainter magnitudes is compatible with the *M* giant infrared results of Frogel & Blanco (1990). They concluded that the $J-K$ color magnitude diagram of the Bar west field is dominated by AGB stars of the kind found in intermediate age clusters whereas only 20% of the AGB population is similar to that found in clusters younger than 100 Myr.

Interpretations of the gap between blue and red clusters, whose nature has been ascribed to several reasons in past studies, must take into account that it is not depleted of clusters, but filled with fainter ones, at least in the Bar region.

The $(U-B)$ vs $(B-V)$ diagram is presented in Fig. 5. Taking all clusters in common between Searle *et al.* (1980, hereafter referred to as SWB) and VDB81, we have defined the boundaries among the different SWB clusters types. These boundaries differ slightly from those in CBB88: (a) we introduce a type for clusters associated to H II regions which we designated SWB 0. (b) We increase the area corresponding to SWB I clusters with the possibility of having red supergiants. The locus of massive LMC clusters with red supergiants is indicated in Fig. 5. Such clusters, as NGC 2004, NGC 2098, and NGC 2100 are characterized by the sudden change of continuum slope in the near infrared by the occurrence of red supergiants around 10 Myr (Bica *et al.* 1990). On the other hand, SL 393 is a small cluster in VDB81 which presents excessively red $B-V$ for its $U-B$ color and has a bright star near its edge. We show in Fig. 5 new observations with and without the star (Table 2). It is clear from the diagram that the color of such small clusters are strongly affected by the presence of a single red supergiant. (c) We split the group SWB IV into IVA (bluer) and IVB (redder). In the SWB Q(*ugr*) vs Q(*vgr*) diagram there are evidences of a degeneracy in this region of the plane since clusters which form a smooth sequence in terms of integrated *UBV* colors and spectral properties are mixed. These evidences are: (i) The color range of group IV is smaller than those of groups III or V in SWB, whereas it is much wider than those of its neighbors in the $U-B$ vs $B-V$ plane. (ii) Degeneracy for SWB IV is suggested by examples such as NGC 1831 and NGC 1783, which were classified by SWB as type V. Nevertheless, integrated spectra of these clusters are drastically different, the former being much bluer (Bica & Alloin 1986a, b). In the latter papers are also presented spectra of NGC 1868, the prototype of a blue/red transition cluster, with spectral properties intermediate between NGC 1831 and NGC 1783. Using *UBV* data from VDB81 our equivalent SWB classification yields for NGC 1831, NGC 1868, and NGC 1783 types IVA, IVB, and V, respectively.

The derived equivalent SWB types for the clusters in the Bar are given in Tables 1, 2, and 3. For clusters in common with SWB, identical SWB types are found in all cases (NGC 1943 is a borderline case). As can be judged from Fig. 5, the $(B-V)$ color is not a good age discriminator owing to the influence of red supergiants on less massive clusters and the $(B-V)$ degeneracy for intermediate age and old clusters (SWB types V to VII) as well as that for blue clusters (SWB I to IVA). The equivalent SWB type is better for that purpose because it takes into account both colors. Consequently its histogram (Fig. 6) is more representative of the history of star cluster formation than that of $(B-V)$ (Fig. 4). The most frequent clusters are of types III and II. An important result is the absence of type VI clusters; we point out that reddening effects would tend to populate this zone. This suggests that at least in the present sample this age group is really absent in the Bar. Reddening estimates for individual clusters in the Bar region exist only for a few of them. Persson *et al.*'s (1983)

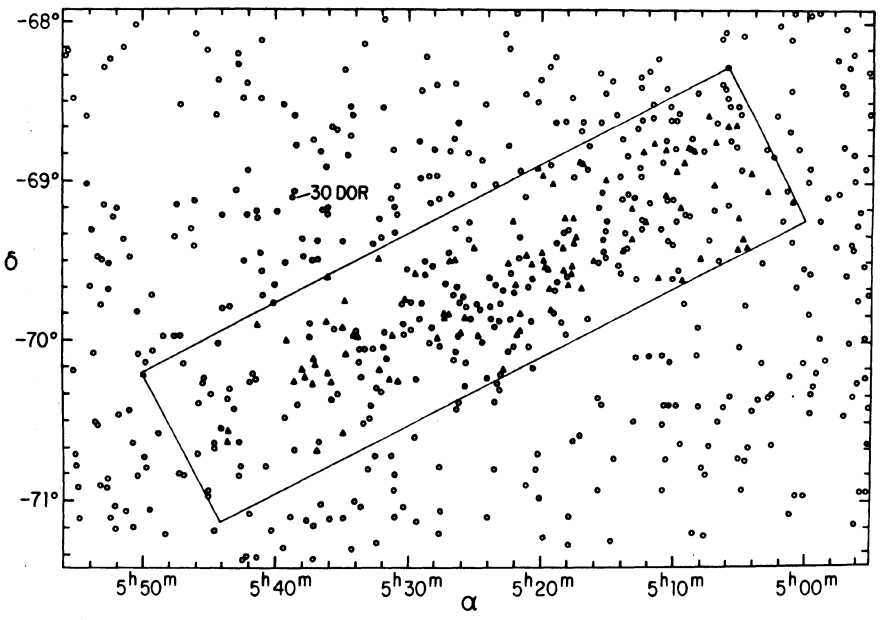

FIG. 1. Spatial distribution of all clusters from the SL (○) and HS (△) catalogs in a 3°×5° central region of the LMC. The rectangle contains the Bar as seen on deep photographic plates. Notice that the cluster density in the Bar is larger. All clusters presented in Tables 1–3 are located within the rectangle.

estimates of foreground plus internal reddening for 13 objects in common provide $E(B-V)=0.16\pm0.04$, with maximum and minimum values respectively for the blue cluster NGC 1856 (0.24) and the type VII cluster NGC 1898 (0.09). Owing to this small number of reddening estimates we have decided to analyze observed colors indicating in Fig. 5, a foreground dereddening vector for $E(B-V)=0.06$. Internal reddening differences throughout the Bar and within young clusters is a source of scatter in Fig. 5. However, it is worth noting that the color scatter is small ($\sigma\approx0.1$) for the very young and very old clusters (SWB 0 and SWB VII, respectively), whereas it is substantially larger for types II to IVA ($\sigma\approx0.25$). In both cases the scatter is larger than photometric errors. The lower value for types 0 and VII would indicate an upper limit for differential reddening, whilst the higher values in the other groups might be associated to stochastic effects in the light contribution from massive AGB stars, which are expected to occur in such SWB types.

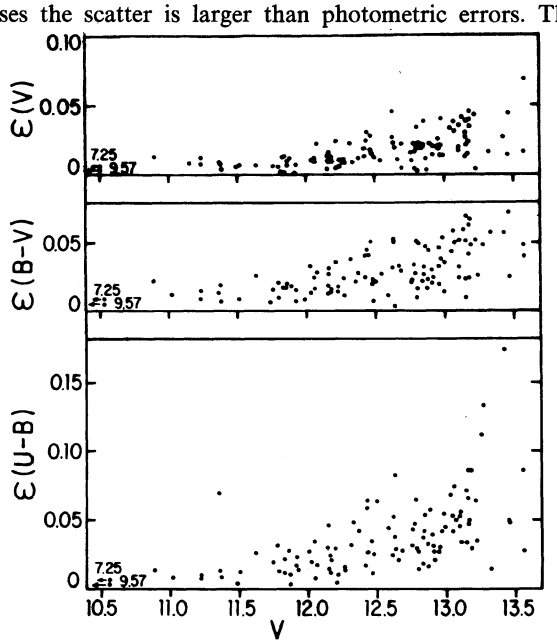

FIG. 2. Behavior of internal errors of the magnitude and colors for the clusters as a function of integrated V magnitude.

3.2 Spatial Distribution of Age Groups

The spatial distribution of very young clusters in the LMC was analysed by Hodge (1973), with ages estimated from bright stars, whereas clusters of all ages were studied by VDB81. The latter sample is, however, very small in the Bar region. The present sample of 129 clusters is suitable for a more conclusive analysis. The spatial distribution of the different SWB types in the Bar is shown in Fig. 7, where we also indicate the corresponding age ranges (Elson & Fall 1985).

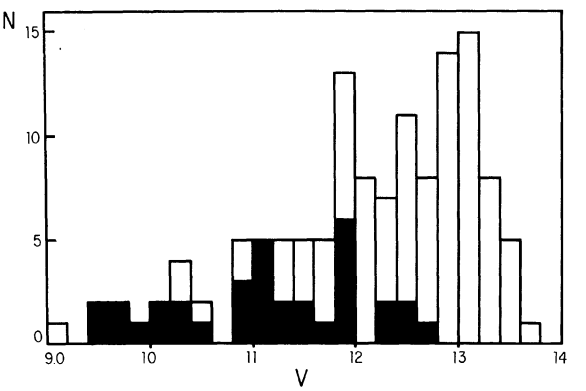

FIG. 3. Histogram of integrated V magnitudes. The dark histogram denotes the sample from the literature and the light one the new sample of observed clusters.

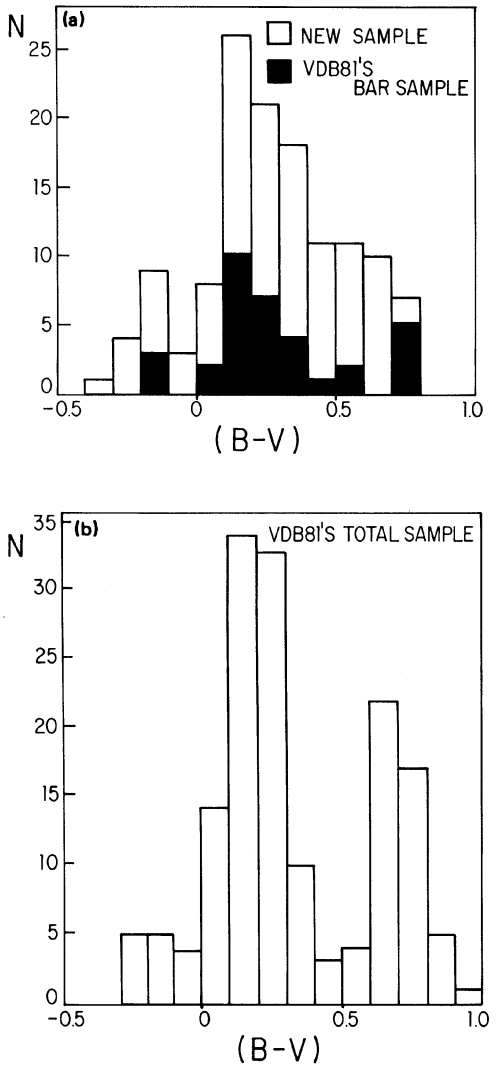

FIG. 4. (a) Histogram of the $(B-V)$ color. Old and new samples as in Fig. 3. Notice that the gap between blue and red clusters disappears with the inclusion of the new sample. (b) The global LMC sample from VDB81 for comparison purposes.

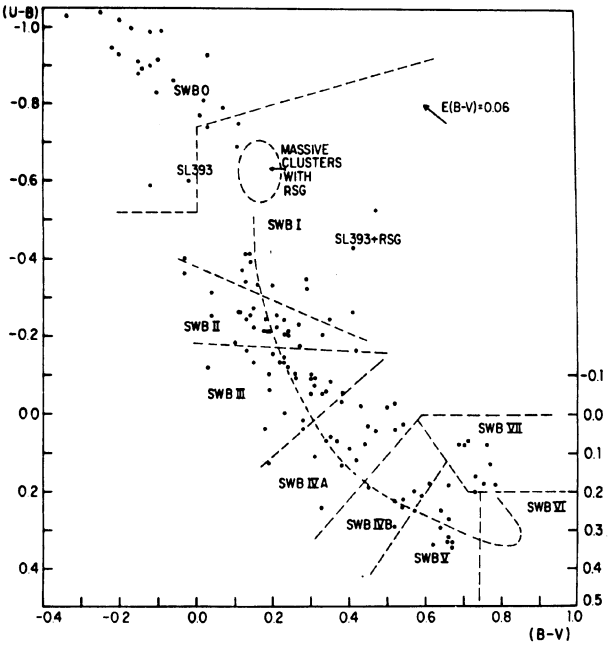

FIG. 5. Color–color diagram. Zones corresponding to the different age groups are indicated. The mean line of clusters from VDB81 is also shown. The colors are observed ones and the effect of a foreground dereddening of $E(B-V)=0.06$ is represented by the arrow. The positions of the cluster SL 393 with and without the red supergiant are labelled.

Figure 7(a) shows the spatial distribution of SWB 0 clusters. Most of them are associated to emission nebulae (Henize 1956), according to the designations in Tables 1 and 2. We also show in the same figure the remaining nebulae from Henize's catalog, which are mostly small H II regions. Figure 7(a) includes essentially all star-forming regions in the LMC Bar. We conclude that their spatial distribution is not homogeneous with an avoidance zone eastward of the center, probably as a consequence of a strong star forming event in a previous generation [SWB III, Fig. 7(c)]. The central and western parts of the Bar appear to have formed more clusters than the eastern one, moreover if one considers that the eastern ridge of H II regions starting at NGC 2079 is probably part of the 30 Dor complex. We recall that 30 Dor (NGC 2070) is located towards north-east of the Bar (Fig. 1) and some of

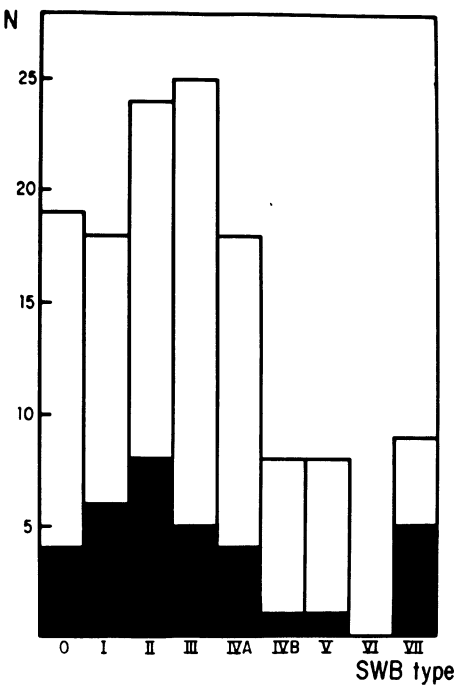

FIG. 6. Histogram of age groups. Old and new sample as in Fig. 3. SWB VI clusters are absent in the Bar.

the H II regions in the southern part of the complex might overlap with the north-east part of the Bar, suggesting even less star formation in the eastern half of the Bar itself. It should be noted that the Bar region is not a present-day intense star-formation site as compared to other regions of the LMC, where the H II regions are more abundant (see, e.g., the deep Hα plates in Davies *et al.* 1976).

Figure 7(b) shows clusters of types SWB I and II, corresponding to the age ranges $10 < t(\mathrm{Myr}) < 30$ and $30 < t(\mathrm{Myr}) < 70$, respectively. It can be seen that there is a strong gradient in the cluster density towards the west. For type III ($70 < t(\mathrm{Myr}) < 200$), a large concentration of clusters appears in the eastern half [Fig. 7(c)]. These are the compact group of clusters formed by NGC 2058, NGC 2065, four small companions and the nearby clusters NGC 2036, NGC 2028, SL 574, and SL 591. This strong coeval concentration shows that a strong star-forming event has occurred in the eastern part of the Bar about 100 Myr ago. This locus is also shown in the panels for younger clusters [Figs. 7(a) and 7(b)]. The time sequence suggests that the strong burst at 100 Myr has inhibited star formation in the eastern part ever since, probably as a consequence of

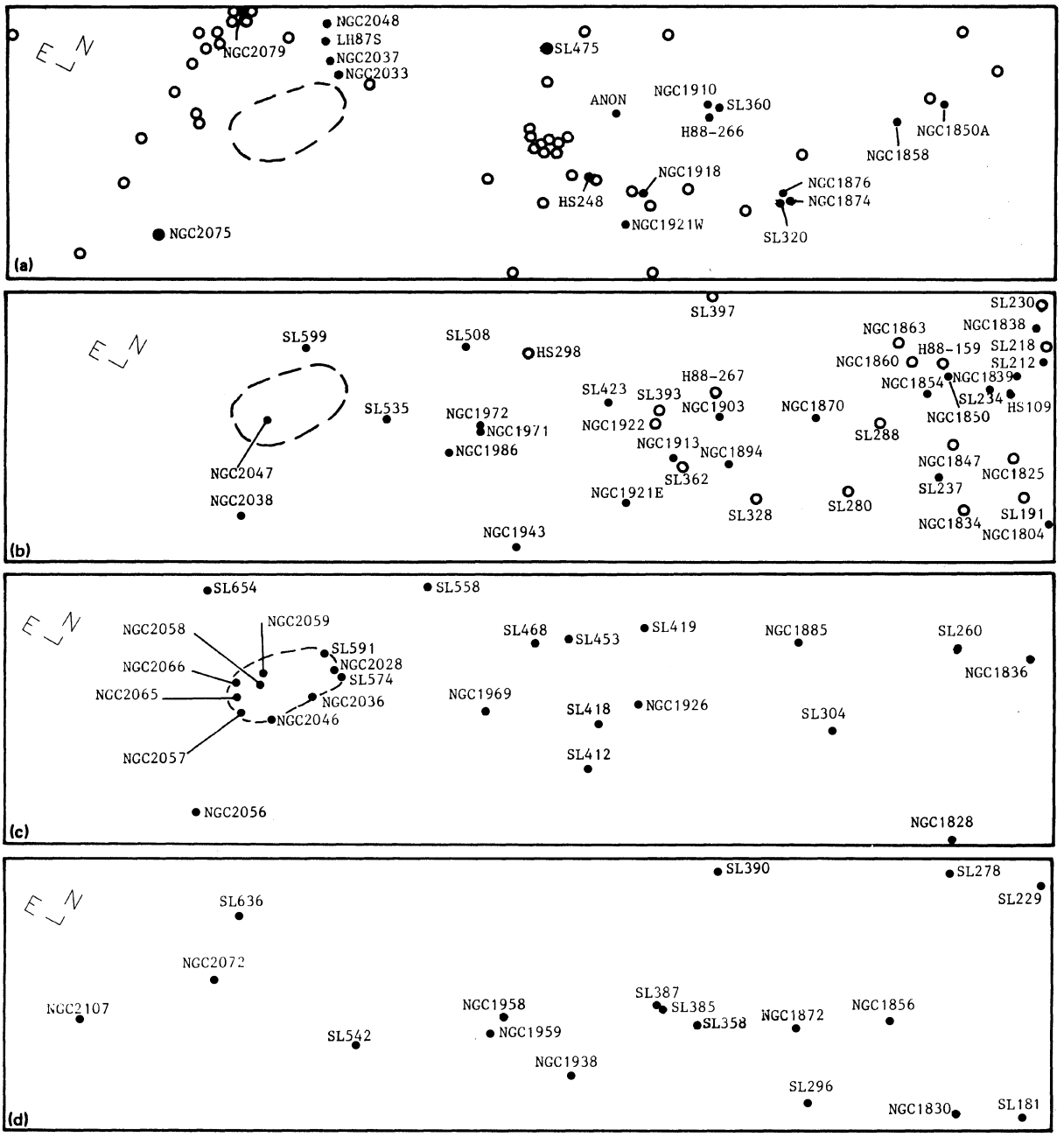

FIG. 7. Spatial distribution of the different age groups: (a) age range in Myr $0 < t < 10$, filled circles are SWB 0 clusters which in most cases are associated to H II regions and open circles are (other) emission nebulae from Henize (1956); (b) open circles are SWB I clusters ($10 < t < 30$) and filled circles are SWB II ($30 < t < 70$); (c) SWB III ($70 < t < 200$), dashed-line encircled zone contains compact group of clusters which is also shown in (a) and (b); (d) SWB IVA ($200 < t < 400$); (e) open circles are SWB IVB ($400 < t < 800$) and filled circles are SWB V ($800 < t < 2000$); (f) SWB VII ($5000 < t < 16000$). The box dimensions are $1° \times 4.2° (0.9 \times 3.8$ kpc).

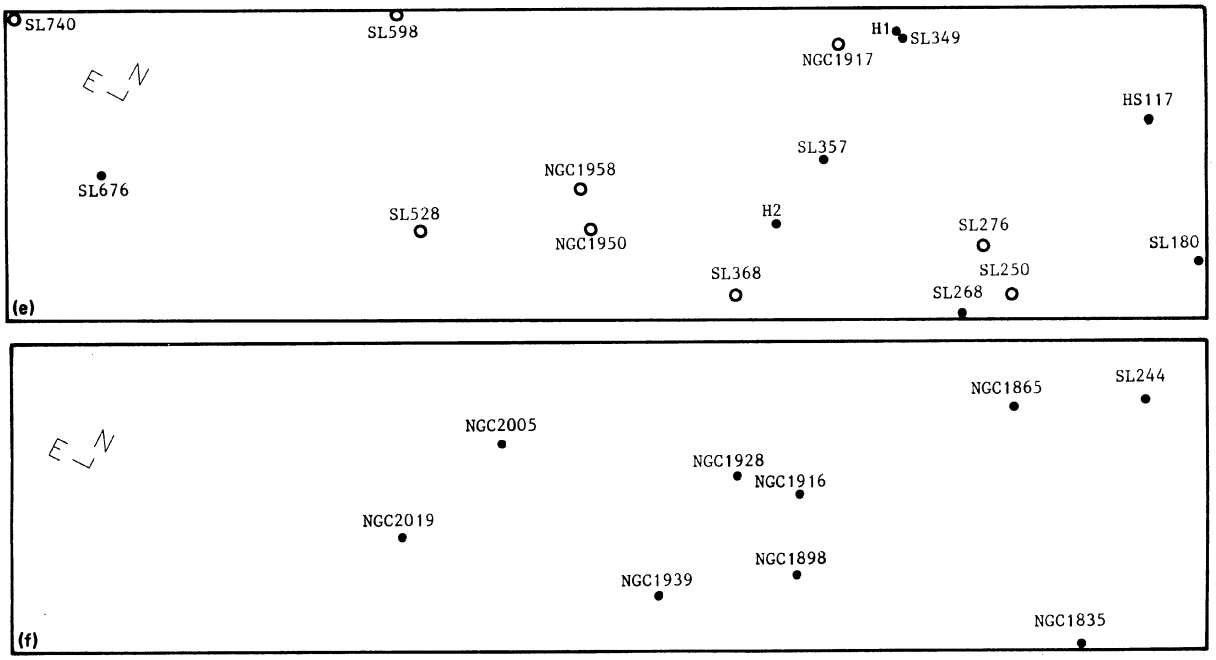

FIG. 7. (continued)

sweeping of the interstellar matter. This effect might have originated the southern part of 30 Dor complex, as an alternative explanation for the appearance of the ridge of H II regions in Fig. 7(a). The present position of older clusters will not be simply related to the position where it was formed.

SWB IVA clusters present a more uniform spatial distribution throughout the Bar [Fig. 7(d)]. Figure 7(e) shows that the older types IVB and V, corresponding to ages $0.4 \leqslant t \leqslant 2$ Gyr, occupy preferentially the western and central parts, which might suggest that the older stars and the larger mass concentrations occur in those regions. In this scenario, the eastern part of the Bar would be a more recent appendix formed mainly at the epoch of SWB III clusters.

In Fig. 7(f) the very old clusters (SWB VII), are probably part of another LMC halo or disk subsystem projected on the Bar, or even some of them might have been trapped in the Bar potential. These scenarios fit the overall LMC kinematics and the few cluster velocities available in the Bar region (Freeman *et al.* 1983; Olszewski *et al.* 1991): five SWB VII clusters provide 242 ± 42 km/s, whereas ten clusters of types SWB I to IVB produce 252 ± 18 km/s.

An intriguing question is that no type VI cluster has been detected in the Bar, although the Poisson statistics is still marginally significant (eight clusters in each adjacent group). If the lack of SWB VI clusters persists for deeper samples a possible explanation could be that the Bar was formed about 2 Gyr ago. Indeed the deepest available HR diagram of the Bar shows a lack of subgiants stars as shown by Hardy *et al.* (1984). A comparison with CMDs of Galactic clusters dated by Janes & Demarque (1983) indicates that as age increases the transition to a populated subgiant branch takes place between clusters like NGC 2420/NGC 2506 and M67, i.e., $t \approx 3$ Gyr. In terms of LMC clusters the Bar field CMD resembles those of SWB V clusters like NGC 2162 (Schommer *et al.* 1984). On the other hand, type VI clusters like NGC 2155 (Hesser *et al.* 1976) already presents a well-developed subgiant branch, as does also the SWB VI/VII cluster ESO 121-SC03 (Mateo *et al.* 1986). It would be important to carry out a systematic survey of velocities and a deeper integrated photometry for Bar clusters in order to clarify these points.

3.3 Cluster Formation Rate

There have been several recent analyses of the age distribution of LMC clusters which are summarized in Elson & Fall (1988, hereafter referred to as EF88). Using similar prescriptions we have derived in Fig. 8 the age distribution for the Bar sample, normalized to the blue cluster distribution. As usual in such discussions we also show Wielen's curve for the Galactic clusters, which shows a strong drop due to cluster dissociation effects.

The Bar sample behavior for the age range $7 \leqslant \log(\tau/\mathrm{yr}) \leqslant 8.5$ is comparable to that of the whole LMC sample according to EF88 and CBB88. For older ages the Bar clusters follow closely CBB88, within the error bars and is located slightly below EF88. However, a fundamental difference with respect to the whole LMC sample is the no detection of type VI clusters, as discussed in Sec. 3.1, which is represented by a discontinuity near $\log(\tau/\mathrm{yr}) \approx 9.5$.

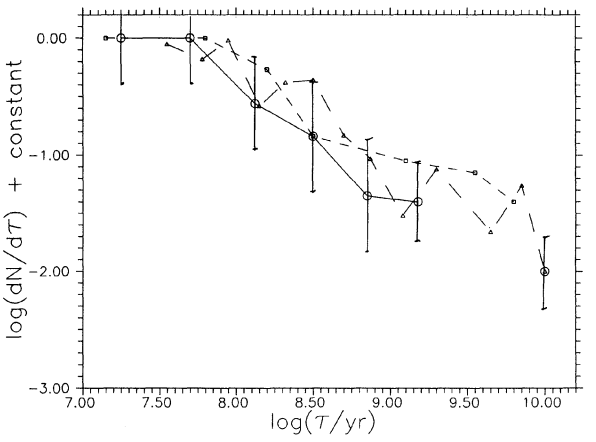

FIG. 8. Cluster formation rate. Circles and full line: Bar sample with error bars according to Poissonian noise. Triangles and dashed line: whole LMC EF88 sample. Squares and short dashed line: whole LMC CBB88 sample. Full line: Wielen's Galactic open cluster sample.

4. PAIRS, TRIOS, AND A COMPACT GROUP OF CLUSTERS: COEVAL?

The present sample of clusters contains eleven close pairs, two trios, and one compact grouping of clusters which are shown in Fig. 9, together with the corresponding SWB types. Bhatia *et al.* (1987) have compared colors of cluster pairs in the LMC in order to check the physical association of the components. We have two pairs in common: NGC 1850/NGC 1850A and NGC 1938/NGC 1939.

Concerning the NGC 1850 system we also find that the compact companion NGC 1850A is bluer, belonging to the SWB 0 group (Table 1). NGC 1850 is SWB II implying an age difference of $\approx$50 Myr. NGC 1850A is certainly responsible for the ionization of the emission nebula Henize 103 in which the clusters are embedded. In addition, we have observed another companion called H88−159 (Hodge 1988), which Bhatia & MacGillivray (1987) had interpreted as a tail resulting from the interaction of NGC 1850 and NGC 1850A; the type for H88-159 is SWB I, i.e, intermediate between NGC 1850 and NGC 1850A, which argues against this scenario. We conclude that NGC 1850, NGC 1850A, and H88−159 could be interpreted as a physical trio with a common origin with star formation spread over 50 Myr.

Since the colors of Bhatia *et al.* (1987) for the pair NGC 1938/NGC 1939 are instrumental they should be taken with caution. We find that these two clusters belong to groups SWB IVA and VII, respectively, implying an age difference of at least 5 Gyr. Isophotal distortions seen in a digitalized ESO B plate image suggest that the clusters are interacting. So the physical association in this case seems to have been originated from encounter. We emphasize that the color difference for the pair has been independently confirmed at CTIO and CASLEO (Table 1). The trio NGC 1969/NGC 1971/NGC 1972, with types III, II, and II, respectively, suggests physical connection with an age dispersion of 50 Myr.

The pairs H1/SL 349, SL 385/SL 387, NGC 2028/SL 574, and NGC 1874/NGC 1876 are coeval because of the coincident SWB type in each pair. The same occurs for the pair NGC 2058/NGC 2059, which in turn is part of a compact grouping of clusters (part of the one discussed in Sec. 3). Eight clusters lie within a 15′×15′ area. Six of them are of type III and one of type II (Fig. 9), which indicates that they are coeval. The only intruder is NGC 2072, which differs from the rest by at least 200 Myr. It will be of great interest to make a detailed dynamical study of this "cluster of clusters." A possible fate is the merging of the system as a result of dynamical friction (White 1979).

The pairs H88−266/H88−267 and NGC 1921E/NGC 1921W have noncoincident SWB types, but the age differences of the components are, respectively, $<$20 Myr and $<$70 Myr, which are almost coeval. The age difference in the pair SL 468/HS 298 may be larger than 100 Myr.

Finally, the pairs SL 229/SL 230, SL 276/SL 280 and NGC 1903/SL 357 have components with different SWB types, which imply in all cases age differences larger than 150 Myr.

5. CONCLUSIONS

The main results of this work are:

(a) Integrated *UBV* photometry of star clusters in the LMC Bar region basically complete up to $V \simeq 13.2$ is presented. The sample includes 95 previously unstudied clus-

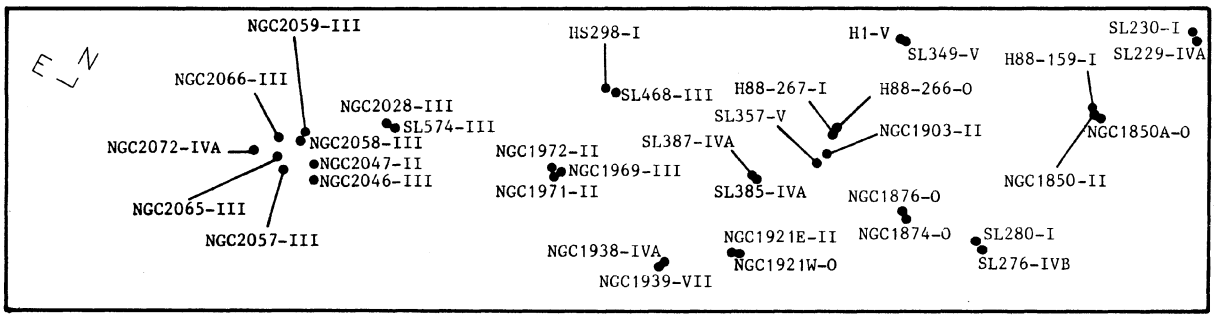

FIG. 9. Pairs, trios, and a compact group of clusters. SWB types are indicated for each component.

ters and revised values for 11 ones, totalling 129 objects with the available observations in the literature.

(b) The extensively discussed $(B-V)$ gap between blue and red clusters in the LMC and SMC as a whole, which also exists for the brighter Bar clusters, vanishes in the Bar with the inclusion of the new observations. This result is compatible with early population studies of the LMC Bar, which have indicated that its typical color is $(B-V)=0.49$.

(c) Age groups in terms of equivalent SWB types are derived and their spatial distribution analyzed. A strong star-forming event in the eastern part of the Bar occurred about 100 Myr ago, as suggested by a large cluster concentration of this age, whereas star cluster formation after this episode has taken place mostly in the western half. Star clusters of type SWB VI are absent in the Bar region.

(d) The possibility of coeval formation was checked in 11 close pairs, 2 trios, and a compact grouping of 8 clusters. We found that only four pairs have not coeval components.

We thank the staffs at CTIO and CASLEO for the hospitality and assistance during the observing runs. This work was partially supported by the brazilian institutions CNP_q and FAPERGS, and the CONICOR from Argentina. We are grateful for an anonymous referee for interesting remarks.

REFERENCES

Alcaino, G., & Liller, W. 1982, A&A, 144, 213
Bhatia, R. K., & MacGillivray, H. T. 1987, ESO Conference Workshop Proceedings No. 27, p. 485
Bhatia, R. K., Cannon, R. D., & Hatzidimitriou, D. 1987, ESO Conference Workshop Proceedings No. 27, p. 489
Bica, E., & Alloin, D. 1986a, A&A, 162, 21
Bica, E., & Alloin, D. 1986b, A&AS, 66, 171
Bica, E., Alloin, D., & Santos, Jr., J. F. 1990, A&A, 235, 103
Bica, E., Dottori, H., & Pastoriza, M. G. 1986, A&A, 156, 261
Chiosi, C., Bertelli, G., & Bressan, A. 1988, A&A, 196, 84
Davies, R. D., Elliot, K. H., & Meaburn, S. 1976, MNRAS, 81, 89
de Vaucouleurs, G., & de Vaucouleurs, A. 1959, PASP, 71, 83
Elson, R., & Fall, S. 1985, ApJ, 299, 211
Elson, R., & Fall, S. 1988, AJ, 96, 1383
Freeman, K. C., Illingworth, G., & Oemler, A. 1983, ApJ, 272, 488
Frogel, A., & Blanco, V. M. 1990, ApJ, 365, 168
Geisler, D. 1987, AJ, 93, 1081
Gordon, K., & Kron, G. 1983, PASP, 93, 461
Graham, J. A. 1982, PASP, 94, 244
Graham, J. A., & Nemec, J. M. 1984, in Structure and Evolution of the Magellanic Clouds, edited by S. Van den Bergh and K. S. Boer (Reidel, Dordrecht), p. 37
Hardy, E., Buonanno, R., Corsi, C. E., Janes, K. A., & Schommer, R. A. 1984, ApJ, 278, 592
Henize, K. 1956, ApJS, 12, 163
Hesser, J. E., Hartwick, F. D. A., & Patricio Ugarte, P. 1976, ApJS, 32, 283
Hodge, P. W. 1960, ApJ, 131, 351
Hodge, P. W. 1961, ApJ, 133, 413
Hodge, P. W. 1973, AJ, 78, 163
Hodge, P. W. 1988, PASP, 100, 1051
Hodge, P. W., & Sexton, J. 1966, AJ, 71, 363
Hodge, P. W., & Wright, F. W. 1967, The Large Magellanic Cloud (Smithsonian Institute, Washington, DC)
Lucke, P. B., & Hodge, P. W. 1970, AJ, 75, 171
Magalhães, A. M., Benedetti, E., & Roland, E. 1984, PASP, 96, 383
Mateo, M. 1987, ESO Conference Workshop Proceedings No. 27, p. 467
Mateo, M., Hodge, P. W., & Schommer, R. A. 1986, ApJ, 311, 113
Mould, J. R., da Costa, G. S., & Crawford, M. D. 1986, ApJ, 304, 265
Olszewski, E. W., Schommer, R. A., Suntzeff, N. B., & Harris, H. C. 1991, AJ, 101, 515
Persson, S. E., Aaronson, M., Cohen, J. G., Frogel, J. A., & Matthews, K. 1983, ApJ, 266, 105
Schommer, R. A., Olszewski, E. W., & Aaronson, M. 1984, ApJ, 285, L53
Searle, L., Wilkinson, A., & Bagnuolo, W. 1980, ApJ, 239, 803
Shapley, H., & Lindsay, E. 1963, IrAJ, 6, 74
Van den Bergh, S. 1981, A&AS, 46, 49
White, S. 1979, MNRAS, 189, 831